Electronic Supplementary Material (ESI) for Nanoscale.

Electronic Supplementary Information

Concentration-Regulated Photon Upconversion and Quenching in $NaYF_4:Yb^{3+}$, Er^{3+} Nanocrystals: Nonexponentiality Revisited

Liyuan Sun, Rongyao Gao, Tingting Pan, Xi-Cheng Ai, Limin Fu* and Jian-Ping Zhang*

Department of Chemistry, Renmin University of China,

Beijing 100872, China

Corresponding author: Tel: +86 010 62516604

*E-mail: lmfu@ruc.edu.cn

*E-mail: jpzhang@ruc.edu.cn

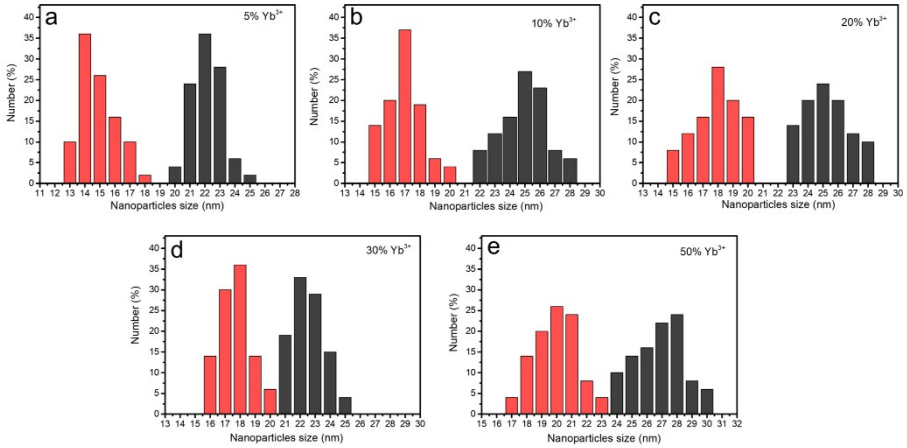

Fig. S1 Size distribution histograms of (a-e) $NaYF_4$:2%Er, xYb (x = 5%, 10%, 20%, 30%, 50%) nanocrystals.

The energy transfer upconversion mechanisms of the green and red emission[1-3]

The transitions of the $^2H_{11/2}/^4S_{3/2} \rightarrow {}^4I_{15/2}$ (green emission) and $^4F_{9/2} \rightarrow {}^4I_{15/2}$ (red emission) of Er^{3+} ions are both two-photon mechanism. The $^4I_{15/2}$ (Er^{3+}) extract two excitation energy photons from the neighbor $^2F_{5/2}$ (Yb^{3+}), producing the $^4F_{7/2}$ (Er^{3+}), followed by the population of the $^2H_{11/2}/^4S_{3/2}$ (Er^{3+}) via non radiative relaxation. The radiative transition from $^2H_{11/2}/^4S_{3/2}$ (Er^{3+}) to $^4I_{15/2}$ (Er^{3+}) leads to green emission. The $^2H_{11/2}/^4S_{3/2}$ (Er^{3+}) extract the third excitation energy photons from the neighbor $^2F_{5/2}$ (Yb^{3+}), producing the $^4G/^2K$ (Er^{3+}), followed by the population of the $^4F_{9/2}$ (Er^{3+}) via BET process. The radiative transition from $^4F_{9/2}$ (Er^{3+}) to $^4I_{15/2}$ (Er^{3+}) leads to red emission.

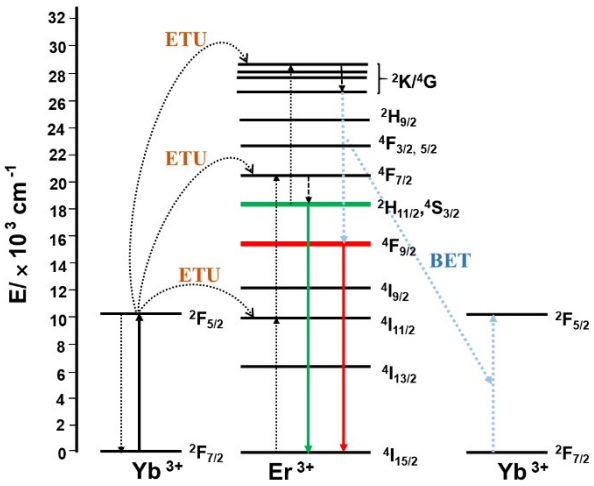

Fig. S2 Diagram of energy transfer upconversion mechanisms of the green and red emission.

Note: ETU = energy transfer upconversion, BET = back energy transfer.

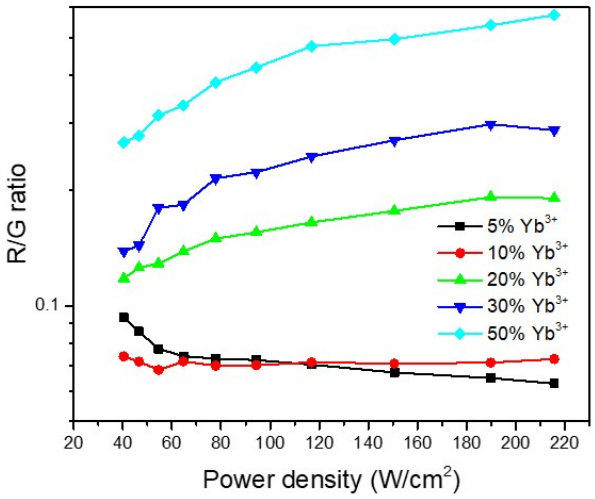

Fig. S3 Plots of R/G ratios of β-$NaYF_4$:2%Er, xYb (x = 5%, 10%, 20%, 30%, 50%) nanocrystals as a function of the excitation power density.

The Kohlrausch function[4-6]

The Kohlrausch function was first applied to the discharge of a capacitor in 1854 by Rudolf Kohlrausch. Williams and Watts in 1970 introduced it in the field of dielectrics. The Kohlrausch function has been found to apply to some luminescence decays of disordered and ordered inorganic solids, semiconductor nanoclusters, single-molecule fluorescence, quantum dot luminescence, and fluorescence lifetime imaging of biological tissues. In fact, the Kohlrausch function can be used to describe decays in the presence of energy transfer.

From a physical perspective, the luminescence decay from a single species, when proportional to its concentration, can be fitted by the Kohlrausch function. Because even if the species has a characteristic lifetime and the decay is ideally exponential, several conformations, microenvironments and quencher spatial configurations around each luminophore will give rise to a distribution of decay rates. This is the case with upconversion luminescence of rare-earth doped nanocrystals.

The Kohlrausch function can be known as follows,

$$I(t) = \exp\left[-\left({}^{t}/_{\tau_0}\right)^{\beta}\right] \tag{S1}$$

where τ_0 is a parameter with the dimensions of time, β represents degree of nonexponentiality. A time-dependent kinetic rate coefficient $k(t)$ for Kohlrausch decay law can

be defined as,

$$k(t) = \frac{\beta}{\tau_0}\left(\frac{t}{\tau_0}\right)^{\beta - 1} \tag{S2}$$

There are three types depending on the value of β: (i) β = 1; the dynamics process is exponential, the kinetic rate coefficient is a constant and τ_0 is the lifetime of whole decay process; (ii) β< 1, the dynamics process is sub-exponential (stretched exponential), the kinetic rate coefficient decreases as the time; (iii) β > 1, the dynamics process is super-exponential (compressed exponential), the kinetic rate coefficient increases as the time. By analyzing the fitting values of β and τ_0, we can obtain the underlying mechanisms of the upconversion population and quenching in rare-earth doped nanocrystals.

The dynamic curves of the prepared nanocrystals with different Yb^{3+} ions doping concentration were fitted by exponential function and Kohlrausch function respectively. Relative fitting formulas were described as follows,

Bi-exponentials fitting:

$$I(t) = \mathrm{A}_1 \exp\left[-\left({}^{t}/_{\tau_1}\right)\right] + \mathrm{A}_2 \exp\left[-\left({}^{t}/_{\tau_2}\right)\right] \tag{S3}$$

Where 1 and 2 represent the rising and decay process respectively.

Bi-Kohlrausch function fitting:

$$I(t) = \mathrm{A}_{rise} \exp\left[-\left({}^{t}/_{\tau_{rise}}\right)^{\beta_{rise}}\right] + \mathrm{A}_{decay} \exp\left[-\left({}^{t}/_{\tau_{decay}}\right)^{\beta_{decay}}\right] \tag{S4}$$

Where rise and decay represent the rising and decay process respectively.

Relative fitting parameters by two fitting formulas above were compared in Table S1 and S2, and the fitting curves were shown in Fig. S3-S11. The fitting results demonstrated that Kohlrausch function fits better than exponential function.

Table S1 Exponential and Kohlrausch function analysis of 540 nm emission

	Exponential fitting				Kohlrausch function fitting					
	A_1	A_2	τ_1 (μs)	τ_2 (μs)	A_{rise}	A_{decay}	τ_{rise} (μs)	τ_{decay} (μs)	β_{rise}	β_{decay}
5% Yb^{3+}	-153.92	154.18	129.33	131.07	-6.10	6.21	187.97	246.74	0.9977	1.1980
10% Yb^{3+}	-327.84	328.06	103.97	104.64	-4.38	4.53	90.91	144.89	1.0481	1.0919
20% Yb^{3+}	-5.04	5.48	60.56	86.89	-5.83	5.99	64.91	93.17	0.9743	1.0323
30% Yb^{3+}	-1.61	2.15	27.92	75.37	-5.78	5.92	31.52	49.80	0.8407	0.87
50% Yb^{3+}	-0.94	1.39	8.63	53.31	-1.38	1.57	7.84	48.16	0.8417	0.9445

Table S2 Exponential and Kohlrausch function analysis of 654 nm emission

	Exponential fitting				Kohlrausch function fitting					
	A_1	A_2	τ_1 (μs)	τ_2 (μs)	A_{rise}	A_{decay}	τ_{rise} (μs)	τ_{decay} (μs)	β_{rise}	β_{decay}
5% Yb^{3+}	-1693.09	30.01	36.38	284.15	-3.23	3.29	113.31	212.57	1.0382	0.8627
10% Yb^{3+}	-204.12	204.11	139.80	141.32	-29.46	29.50	128.08	137.57	1.0339	1.0162
20% Yb^{3+}	-33.04	9.11	66.76	168.88	-2.74	2.78	75.59	174.14	1.0780	1.0148
30% Yb^{3+}	-1.30	1.63	32.35	143.76	-1.59	1.68	33.11	144.97	1.0718	0.9975
50% Yb^{3+}	-1.24	1.22	15.19	175.46	-1.20	1.31	16.29	160.75	0.9802	0.9299

The dynamic curves of 654 nm emission of the prepared nanocrystals were also fitted by three and four exponentials. Fitting formulas were described as follows,

Three exponentials analysis:

$$I(t) = \mathrm{A}_1 \exp\left[-\left(t/\tau_1\right)\right] + \mathrm{A}_2 \exp\left[-\left(t/\tau_2\right)\right] + \mathrm{A}_3 \exp\left[-\left(t/\tau_3\right)\right] \quad \text{(S5)}$$

Four exponentials analysis:

$$I(t) = \mathrm{A}_1 \exp\left[-\left(t/\tau_1\right)\right] + \mathrm{A}_2 \exp\left[-\left(t/\tau_2\right)\right] + \mathrm{A}_3 \exp\left[-\left(t/\tau_3\right)\right] + \mathrm{A}_4 \exp\left[-\left(t/\tau_4\right)\right] \quad \text{(S6)}$$

Relative fitting parameters were shown in Table S3 and S4. The results demonstrated that multi-exponentials analysis does not apply to the rare-earth doped UCNPs.

Table S3 Three Exponentials analysis of 654 nm emission

	A_1	A_2	A_3	τ_1 (μs)	τ_2 (μs)	τ_3 (μs)
5% Yb^{3+}	-4.50	-2.44	2.44	0.31	119.96	278.94
10% Yb^{3+}	666.64	-638.03	-28.61	158.82	157.30	182.02
20% Yb^{3+}	0.94	-3.36	3.46	0.71	80.73	158.68
30% Yb^{3+}	-82.79	81.92	1.34	48.22	48.58	153.23
50% Yb^{3+}	-0.45	-35.90	37.03	17.94	170.62	170.94

Table S4 Four Exponentials analysis of 654 nm emission

	A_1	A_2	A_3	A_4	τ_1 (μs)	τ_2 (μs)	τ_3 (μs)	τ_4 (μs)
5% Yb^{3+}	-10.50	130.74	-124.78	4.53	169.83	249.41	256.53	349.62
10% Yb^{3+}	-3.48	1.35	-157.26	159.37	132.73	57.12	126.84	129.50
20% Yb^{3+}	1.74	-3.67	-22.12	23.99	123.89	77.28	222.95	219.89
30% Yb^{3+}	-1.37	114.51	-112.68	-0.41	28.03	197.36	197.36	358.01
50% Yb^{3+}	-2.12	-0.89	-49.87	51.19	11.30	20.40	158.15	158.60

Kohlrausch function analysis were finally used to explore the specific mechanisms on population and quenching regulated by doping concentration of the sensitizers. In order to ensure the accuracy of fitting, each dynamic data was repeated four times. The fitting results with error bar were shown in Table S5 and S6.

Table S5 Kohlrausch function analysis of 540 nm emission

	τ_{rise} (μs)	τ_{decay} (μs)	β_{rise}	β_{decay}
5% Yb^{3+}	124.93±42.02	219.27±56.82	0.9601±0.06	1.1718±0.19
10% Yb^{3+}	97.49±7.10	145.93±2.24	1.0580±0.01	1.1060±0.01
20% Yb^{3+}	62.90±5.22	90.08±2.54	0.9633±0.01	1.0070±0.02
30% Yb^{3+}	25.44±7.73	67.77±22.08	0.8622±0.02	0.9772±0.13
50% Yb^{3+}	8.25±0.61	45.43±4.00	0.8638±0.05	0.9194±0.05

Table S6 Kohlrausch function analysis of 654 nm emission

	τ_{rise} (μs)	τ_{decay} (μs)	β_{rise}	β_{decay}
5% Yb^{3+}	119.38±15.96	262.89±104.01	1.0699±0.07	1.0123±0.22
10% Yb^{3+}	127.17±0.07	151.40±12.55	1.0686±0.03	1.0354±0.02
20% Yb^{3+}	78.21±11.69	154.77±20.86	1.0562±0.03	0.9534±0.05
30% Yb^{3+}	34.43±1.05	138.96±11.21	1.0407±0.02	0.9724±0.05
50% Yb^{3+}	16.30±0.77	172.06±14.75	1.0080±0.03	0.9860±0.06

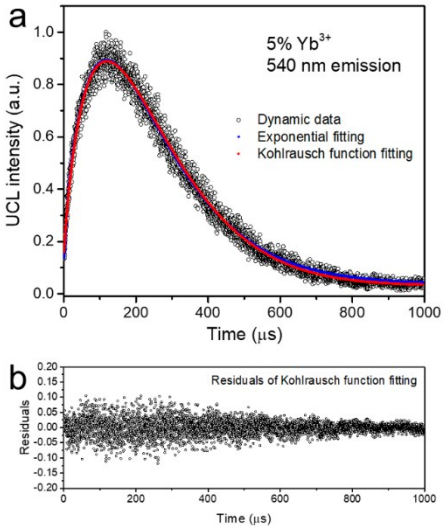

Fig. S4 (a) UCL dynamic data of 540 nm emission of β-$NaYF_4$:2%Er,5%Yb nanocrystals (Black). Fitting curve by the exponential function of the dynamic data (Blue). Fitting curve by the Kohlrausch function of the dynamic data (Red). (b) The residuals of the fitting curve by the Kohlrausch function.

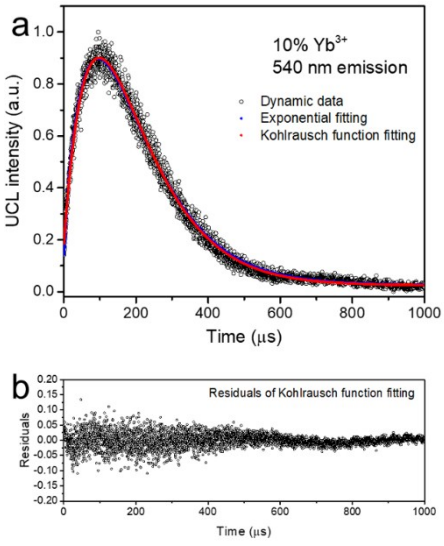

Fig. S5 (a) UCL dynamic data of 540 nm emission of β-$NaYF_4$:2%Er,10%Yb nanocrystals (Black). Fitting curve by the exponential function of the dynamic data (Blue). Fitting curve by the Kohlrausch function of the dynamic data (Red). (b) The residuals of the fitting curve by the Kohlrausch function.

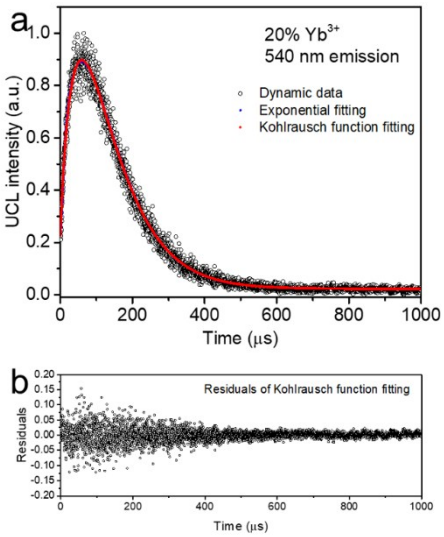

Fig. S6 (a) UCL dynamic data of 540 nm emission of β-$NaYF_4$:2%Er,20%Yb nanocrystals (Black). Fitting curve by the exponential function of the dynamic data (Blue). Fitting curve by the Kohlrausch function of the dynamic data (Red). (b) The residuals of the fitting curve by the Kohlrausch function.

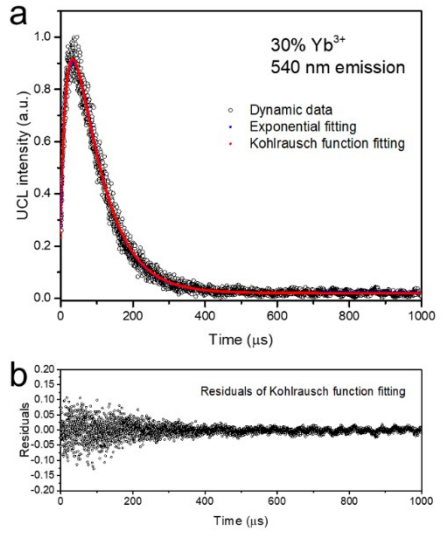

Fig. S7 (a) UCL dynamic data of 540 nm emission of β-$NaYF_4$:2%Er,30%Yb nanocrystals (Black). Fitting curve by the exponential function of the dynamic data (Blue). Fitting curve by the Kohlrausch function of the dynamic data (Red). (b) The residuals of the fitting curve by the Kohlrausch function.

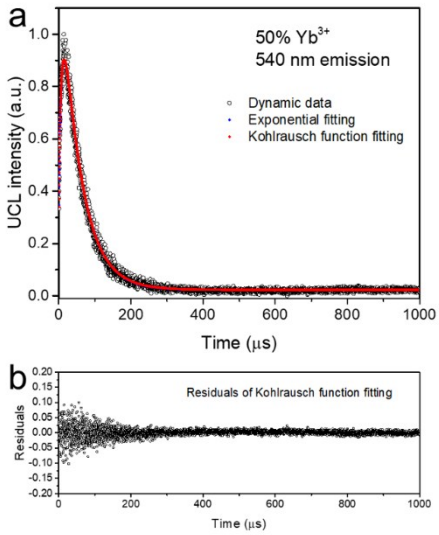

Fig. S8 (a) UCL dynamic data of 540 nm emission of β-$NaYF_4$:2%Er,50%Yb nanocrystals (Black). Fitting curve by the exponential function of the dynamic data (Blue). Fitting curve by the Kohlrausch function of the dynamic data (Red). (b) The residuals of the fitting curve by the Kohlrausch function.

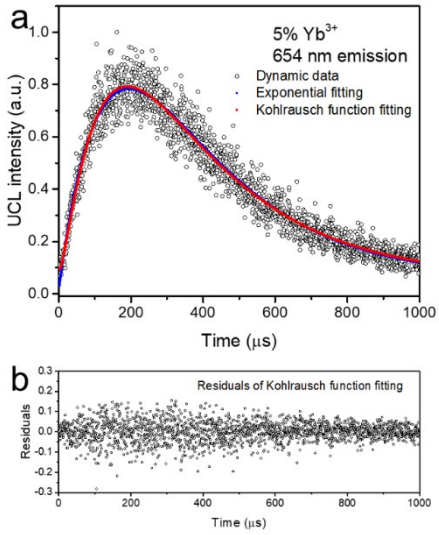

Fig. S9 (a) UCL dynamic data of 654 nm emission of β-$NaYF_4$:2%Er,5%Yb nanocrystals (Black). Fitting curve by the exponential function of the dynamic data (Blue). Fitting curve by the Kohlrausch function of the dynamic data (Red). (b) The residuals of the fitting curve by the Kohlrausch function.

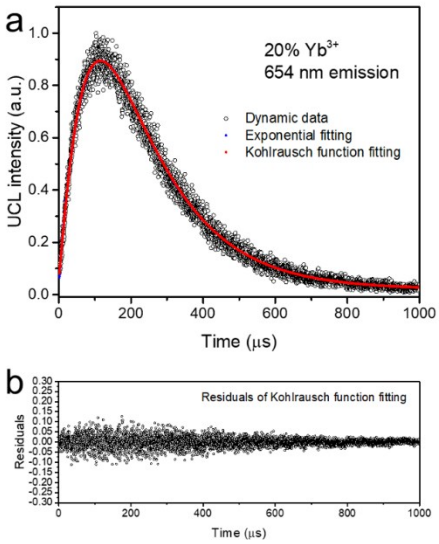

Fig. S10 (a) UCL dynamic data of 654 nm emission of β-$NaYF_4$:2%Er,20%Yb nanocrystals (Black). Fitting curve by the exponential function of the dynamic data (Blue). Fitting curve by the Kohlrausch function of the dynamic data (Red). (b) The residuals of the fitting curve by the Kohlrausch function.

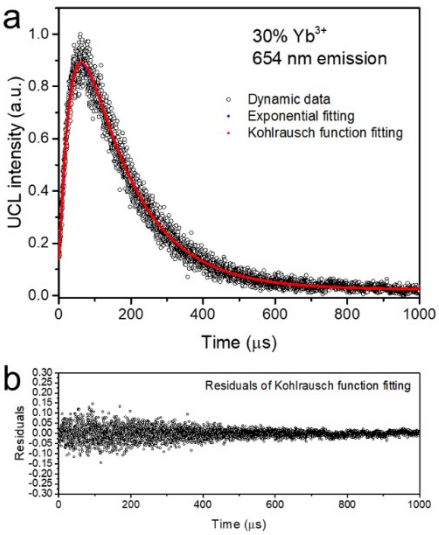

Fig. S11 (a) UCL dynamic data of 654 nm emission of β-$NaYF_4$:2%Er,30%Yb nanocrystals (Black). Fitting curve by the exponential function of the dynamic data (Blue). Fitting curve by the Kohlrausch function of the dynamic data (Red). (b) The residuals of the fitting curve by the Kohlrausch function.

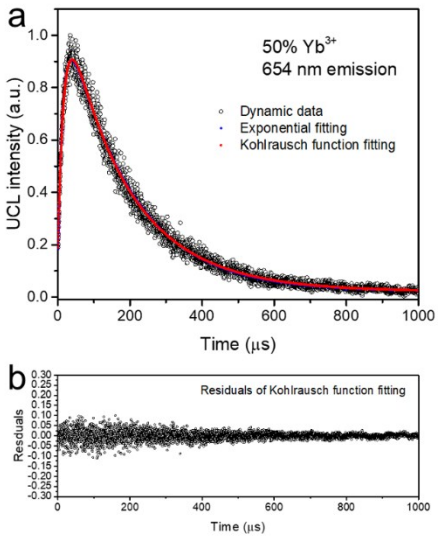

Fig. S12 (a) UCL dynamic data of 654 nm emission of β-$NaYF_4$:2%Er,50%Yb nanocrystals (Black). Fitting curve by the exponential function of the dynamic data (Blue). Fitting curve by the Kohlrausch function of the dynamic data (Red). (b) The residuals of the fitting curve by the Kohlrausch function.

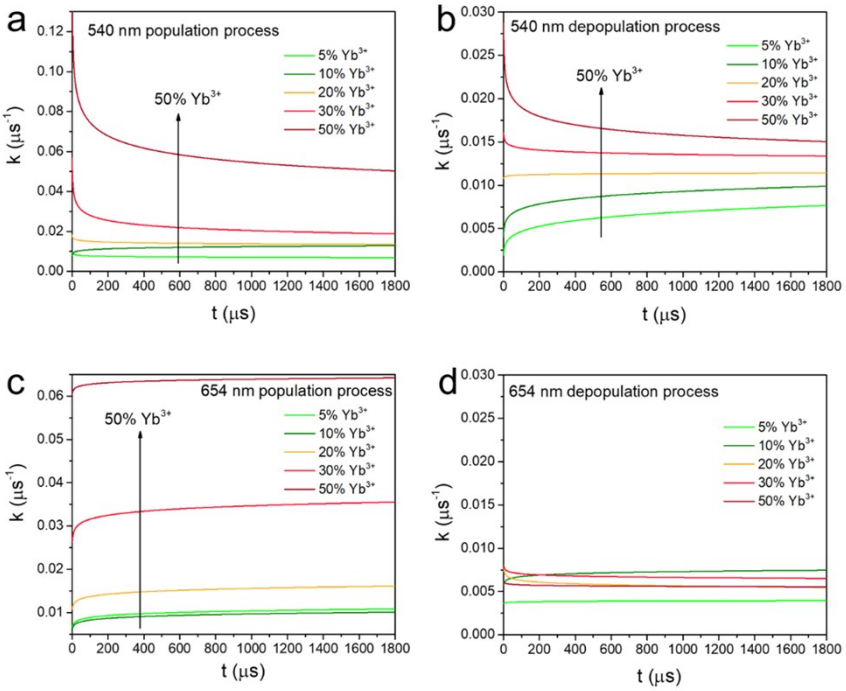

Fig. S13 Kinetic rate coefficients as a function of time of (a) population and (b) depopulation processes of 540 nm emission, and (c) population and (d) depopulation processes of 654 nm emission of β-$NaYF_4$:2%Er, xYb (x = 5%, 10%, 20%, 30%, 50%) nanocrystals.

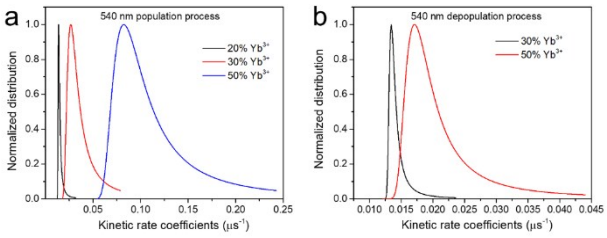

Fig. S14 Normalized kinetic rate coefficients distribution of 540 nm emission (a) population and (b) depopulation process.

References

1. M. T. Berry and P. S. May, *J. Phys. Chem. A*, 2015, **119**, 9805-9811.
2. M. Haase and H. Schafer, *Angew. Chem. Int. Ed.*, 2011, **50**, 5808-5829.
3. L. Li, N. Zhao, L. Fu, J. Zhou, X. Ai and J. Zhang, *Nano Res.*, 2018, **11**, 2104-2115.
4. M. N. Berberan-Santos and B. Valeur, *J. Lumin.*, 2007, **126**, 263-272.
5. M. N. Berberan-Santos, E. N. Bodunov and B. Valeur, *Chem. Phys.*, 2005, **315**, 171-182.
6. T. Palmeira and M. N. Berberan-Santos, *Chem. Phys.*, 2014, **445**, 14-20.